



Synthesis and luminescence of sub-micron sized $\text{Ca}_3\text{Sc}_2\text{Si}_3\text{O}_{12}:\text{Ce}$ green phosphors for white light-emitting diode and field-emission display applications

Yuanhong Liu^{a,b}, Weidong Zhuang^{a,*}, Yunsheng Hu^a, Wengui Gao^a, Jianhua Hao^{b,**}

^a National Engineering Research Center for Rare Earth Materials, General Research Institute for Nonferrous Metals, and Grirem Advanced Materials Co., Ltd., Beijing 100088, PR China

^b Department of Applied Physics, The Hong Kong Polytechnic University, Hong Kong, PR China

ARTICLE INFO

Article history:

Received 5 February 2010

Received in revised form 31 May 2010

Accepted 1 June 2010

Available online 11 June 2010

Keywords:

Luminescence

Green-emitting phosphors

White LED

FED

Rare earths

ABSTRACT

$\text{Ca}_3\text{Sc}_2\text{Si}_3\text{O}_{12}:\text{Ce}^{3+}$ phosphors with sub-micron size were successfully synthesized by a gel-combustion method. The crystal structure and morphology of the phosphors and their photoluminescence were investigated. The results indicate that the pure phase of $\text{Ca}_3\text{Sc}_2\text{Si}_3\text{O}_{12}$ can be obtained at 1100 °C of firing temperature. The particles of phosphor are basically spherical in shape with the mean size less than 1 μm. The grain of the phosphor grows up gradually with the increasing of the firing temperature. The excitation spectrum shows a broad and strong absorption band centered around 450 nm, compatible with the excited wavelength of commercial blue light-emitting diode (LED) for white LED lighting. Bright green-emission located at 505 nm is observed and the intensity of the green-emission increases with the increase of firing temperature. Additionally, under low-voltage (2.5 kV) excitation of electron beam, bright green cathodoluminescence (CL) is also observed, which is attributed to the characteristic emission from Ce^{3+} . Our work suggests that $\text{Ca}_3\text{Sc}_2\text{Si}_3\text{O}_{12}:\text{Ce}^{3+}$ phosphors are promising for both white LED and field-emission display applications.

© 2010 Elsevier B.V. All rights reserved.

1. Introduction

White light-emitting diodes (LEDs) are expected to be useful as environmentally friendly lighting systems for energy saving, long lifetime and safety [1–3]. Recently, white LEDs have also been applied as back-light units in liquid crystal displays and other types of displays. The most widely used white LED consists of a high performance InGaN LED and YAG:Ce yellow phosphor [4–5]. However, this type of white LED lacks red and green light, which causes high color temperature and low color rendering index. These problems could be solved by mixing green and red phosphors instead of single YAG:Ce³⁺ phosphor.

Shimomura and Kijima [6] reported to synthesize a novel green phosphor of $\text{Ca}_3\text{Sc}_2\text{Si}_3\text{O}_{12}:\text{Ce}^{3+}$ with high quantum efficiency and thermal stability by solid-state reaction method [7,8]. A single phase of $\text{Ca}_3\text{Sc}_2\text{Si}_3\text{O}_{12}$ phosphor has been synthesized by gel-combustion method in our previous work [9]. The gel-combustion method has lots of advantages such as a usage of inexpensive precursors, facile operation, low firing temperature, energy efficiency and small particles with narrow size distribution in the obtained product. In addition to the photoluminescence (PL), in our ear-

lier reports the cathodoluminescence (CL) and electroluminescence (EL) properties of materials were found to be essential for field-emission displays (FEDs) and EL displays, respectively, [10–12] which are promising emissive displays realizing high resolution and low consumption of electric power. Low-voltage CL properties of $\text{Ca}_3\text{Sc}_2\text{Si}_3\text{O}_{12}:\text{Ce}^{3+}$ have not been reported so far. Phosphors used in FEDs require several new properties, such as high CL efficiency under low excitation voltage (≤ 5 kV) and specific morphology and surface conditions [13]. In this work, $\text{Ca}_3\text{Sc}_2\text{Si}_3\text{O}_{12}:\text{Ce}$ green phosphor with sub-micron size and basically spherical grain was successfully synthesized by adjusting the firing temperature and using H_3BO_3 flux in gel-combustion method. The phase structure and morphology of the phosphors at different firing temperatures were analyzed by X-ray diffraction (XRD) and scanning electron microscopy (SEM), respectively. The PL, lifetime and CL characteristics of the phosphors were also investigated.

2. Experimental

2.1. Raw materials

Tetraethoxysilane (TEOS 98.5%, International Laboratory, USA), H_3BO_3 (98.5%, Advanced Technology Co., Ltd.), $\text{Ca}(\text{NO}_3)_2 \cdot 4\text{H}_2\text{O}$ (98.5%, Advanced Technology Co., Ltd.), $\text{Ce}(\text{NO}_3)_2 \cdot 6\text{H}_2\text{O}$ (99.9%, International Laboratory, USA), anhydrous ethanol (99.8%, Advanced Technology Co., Ltd.), Sc_2O_3 (99.99%, Shanghai Yuelong New Materials Co., Ltd.) and urea (99.0%, Farco Chemical) were used as starting materials.

* Corresponding author. Tel.: +86 10 82241880; fax: +86 10 62355405.

** Corresponding author. Tel.: +852 27664098; fax: +852 23337629.

E-mail addresses: wdzhuang@126.com (W. Zhuang), apjjhao@polyu.edu.hk (J. Hao).

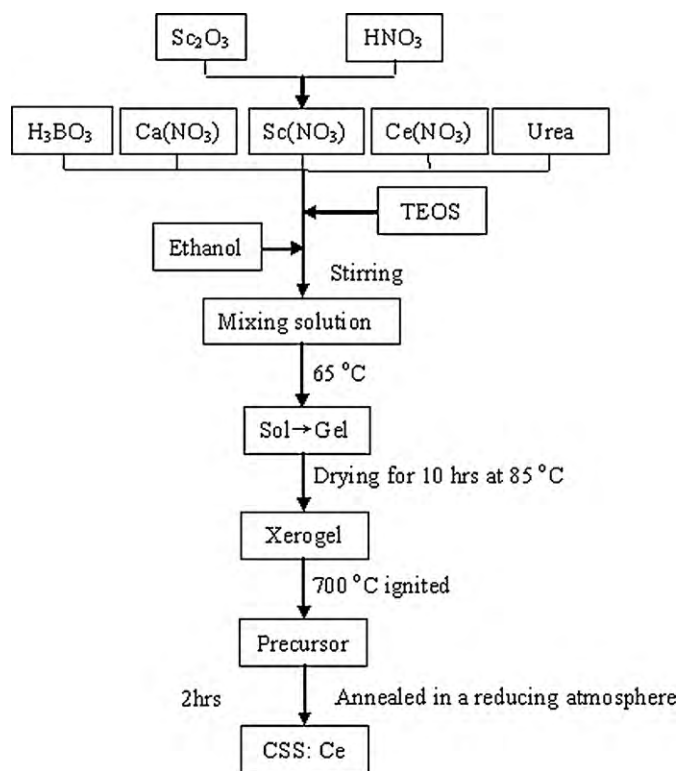


Fig. 1. The synthetic procedure of $\text{Ca}_3\text{Sc}_2\text{Si}_3\text{O}_{12}:\text{Ce}$ green phosphor.

2.2. Preparation of phosphor powder

The synthetic procedure of $\text{Ca}_3\text{Sc}_2\text{Si}_3\text{O}_{12}:\text{Ce}$ green phosphor by a gel-combustion method is presented in Fig. 1. Firstly, Sc_2O_3 was dissolved in an appropriate nitric acid to form nitrate solution. Then, stoichiometric $\text{Ca}(\text{NO}_3)_2 \cdot 4\text{H}_2\text{O}$, $\text{Ce}(\text{NO}_3)_3 \cdot 6\text{H}_2\text{O}$, and $\text{Sc}(\text{NO}_3)_3$ solutions were mixed in a crucible. Appropriate amounts of TEOS, anhydrous ethanol and H_3BO_3 were added into the crucible and continuously stirred for half an hour. The resulted solution was heated at 65°C for 10 h in a dry oven so that superfluous water was evaporated, gradually polymerized into a transparent gel, and dried at 85°C to obtain xerogel. The xerogel was ignited at 700°C in a muffle furnace. The xerogel was simultaneously burnt in a self-propagating combustion manner until the dry sponge sample so-called precursor was formed. Finally, the precursor was fired in a muffle furnace in carbon monoxide mixing gas produced by active carbon at high temperature at different temperature for 2 h to obtain green-emitting phosphor of $\text{Ca}_3\text{Sc}_2\text{Si}_3\text{O}_{12}:\text{Ce}^{3+}$.

2.3. Characterization of phosphor powders

The crystal structure determination of the powder was carried out using a Bruker D8 X-ray diffractometer operating at 40 kV and 40 mA with $\text{CuK}\alpha$ radiation. The PL lifetime, excitation, and emission spectra were obtained with a FLS920P Edinburgh Instruments apparatus.

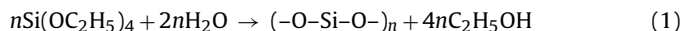
3. Results and discussion

3.1. X-ray diffraction analysis

XRD analysis was used to determine the crystal structure and morphology of the phosphors. As shown in Fig. 2, obvious diffraction peaks corresponding to $\text{Ca}_3\text{Sc}_2\text{Si}_3\text{O}_{12}$ phase were observed in the samples fired at 900°C . The impurity phase in the XRD patterns of the phosphor could be SiO_2 . The existence of the impurity in Fig. 2 is due to the use of low processing temperature at which the pure phase of $\text{Ca}_3\text{Sc}_2\text{Si}_3\text{O}_{12}$ crystal cannot be formed completely. As the firing temperature increases, the intensity of diffraction peak increases, suggesting the improved crystallization of the material. An improvement in crystallinity is in favor of an enhancement of PL intensity from the phosphor as shown in later section. The XRD pattern of the sample fired at 1100°C agrees

with the powder data of $\text{Ca}_3\text{Sc}_2\text{Si}_3\text{O}_{12}$ with a garnet-type structure (space group $la3d$, cubic system) in PDF card (No. 72-1969) [14]. Compared with other synthesis methods, pure $\text{Ca}_3\text{Sc}_2\text{Si}_3\text{O}_{12}$ phase can be obtained at a relatively low temperature of 1100°C by gel-combustion method. Possible mechanism behind the process at low temperature is related to the use of metal nitrates and TEOS rather than oxides of the raw materials in our gel-combustion method.

In the gel-combustion method, a gel network can be formed during the hydrolysis of TEOS as below.



The metal ions in the solution could also be involved in this Si–O gel network, and consequently an atomic-scale mixing is preserved. Therefore, the $\text{Ca}_3\text{Sc}_2\text{Si}_3\text{O}_{12}$ compound obtained by gel-combustion method is single phase and no impurity phase such as Sc_2O_3 was observed as shown in Fig. 2.

The SEM images as shown in Fig. 3 illustrate morphology of the samples fired at different temperatures. It can be seen from Fig. 3(a) that the particles of the sample fired at 900°C are fine and uniform, with an average grain size of 200 nm. It can be seen that grains tend to agglomerate at 1000°C . With further increase in firing temperature, the grains of the sample grow gradually. The particles of the sample fired at 1100°C are dispersing well. The average size of grains is less than $1\ \mu\text{m}$. Phosphors with narrow size distribution and non-agglomeration can make better slurry property and more uniform distribution of light intensity. Furthermore, phosphor particles with spherical shape can decrease the scattering of light and make high packing densities [15,16]. With further increasing of firing temperature or keeping more hours at high temperature, the product becomes hard and needs further grinding, which can make much deficiencies. Accordingly, the luminescence intensity of the phosphor becomes weaker.

The possible mechanism to obtain sub-micron sized phosphor here may be due to a large volume of decomposed gasses during the exothermic redox reaction between metal nitrate and urea as an oxidizing agent and reducing agent, respectively. In addition, the interconnected particles could be broken with the decomposed gasses. On the other hand, low temperature process in gel-combustion method would be helpful to restrain the aggregation of the particles in the phosphors.

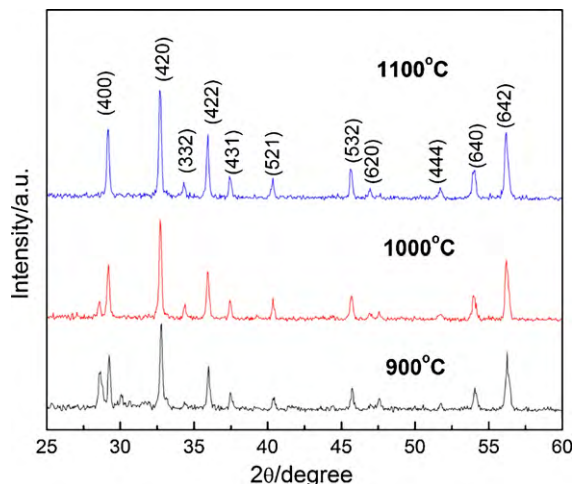


Fig. 2. X-ray diffraction patterns of the samples fired at different temperatures.

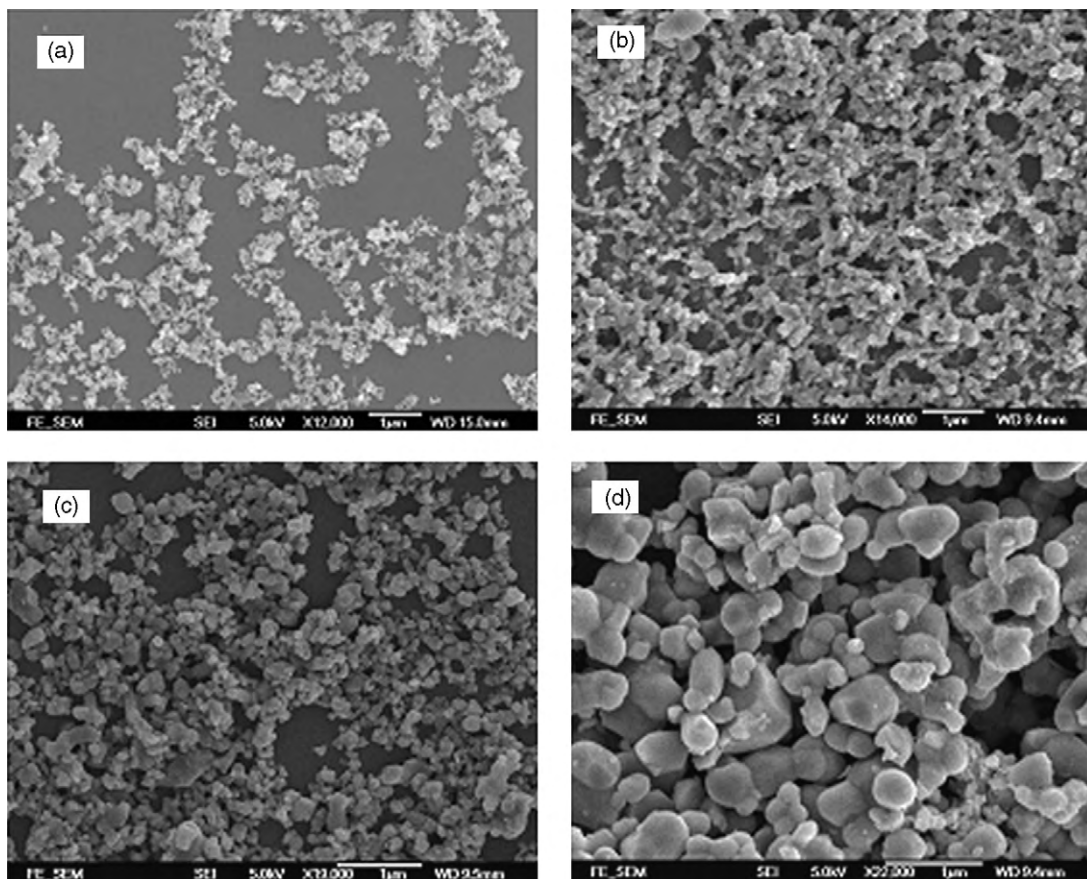


Fig. 3. SEM images of the samples fired at (a) 900 °C, (b) 1000 °C, (c) 1050 °C, (d) 1100 °C.

3.2. Spectral analysis

Fig. 4 shows the PL excitation and emission spectra of the $\text{Ca}_3\text{Sc}_2\text{Si}_3\text{O}_{12}:\text{Ce}$ samples prepared at different firing temperatures. As shown in Fig. 4, the most intense excitation band located at wavelength of 400–500 nm, which suggests that the obtained phosphor is very suitable for the use of a color converter in white LED excited by a commercial InGaN blue LED. There is a broad emission peak around 505 nm in the PL spectra. $\text{Ca}_3\text{Sc}_2\text{Si}_3\text{O}_{12}$ has a garnet-type structure. The Ce^{3+} ions replace the position of Ca^{2+} ions, which

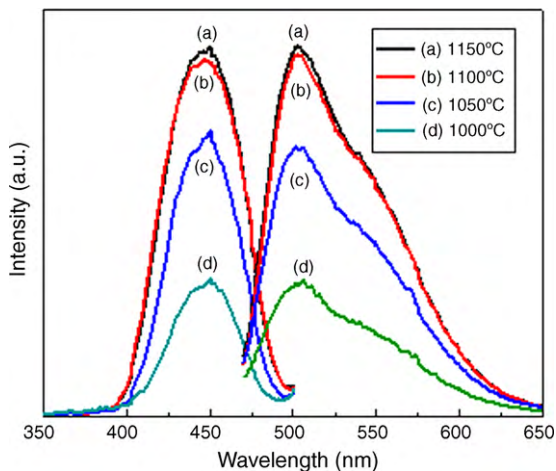


Fig. 4. PL excitation and emission spectra of the $\text{Ca}_3\text{Sc}_2\text{Si}_3\text{O}_{12}:\text{Ce}$ samples at different firing temperatures.

is surrounded by eight O^{2-} ions and occupies the dodecahedron site of the lattice. Due to 4f–5d transition of Ce^{3+} , a broad emission peak around 505 nm was obtained in the PL spectra. This asymmetric green-emission can be decomposed into two Gaussian bands corresponding to the $5d-^2F_{5/2}$ and $5d-^2F_{7/2}$ transitions [9,17–19]. The peak location in both excitation and emission spectra remains basically unchanged with the increase of the firing temperature. This is because the crystal particle size does not affect the photon energy by the transition of 5d–4f transition of Ce^{3+} . However, the luminescence intensity in both excitation and emission spectra increased with the increase of the firing temperature. Because the smaller particle size could generate more surface defects, particularly in oxide based materials [13,20]. Therefore, the PL intensity of the phosphors decreases accordingly. It could be suggested that the PL intensity increased with an increase of crystallinity as well as crystal size as shown in Fig. 3.

To examine the feasibility of the as-synthesized powders as FED phosphors, low-voltage CL spectrum of $\text{Ca}_3\text{Sc}_2\text{Si}_3\text{O}_{12}:\text{Ce}^{3+}$ powder fired at 1100 °C was measured as shown in Fig. 5. The spectrum was measured at room temperature using electron beam with voltage of 2.5 kV as an excitation source. A broad emission peak located at wavelength of 480–650 nm was observed, which is attributed to the characteristic emissions from $5d-^2F_{5/2}$ and $5d-^2F_{7/2}$ transitions of Ce^{3+} . The main peak of emission is located at 505 nm; therefore, green light is observed from $\text{Ca}_3\text{Sc}_2\text{Si}_3\text{O}_{12}:\text{Ce}^{3+}$ sample. The electron penetration depth can be obtained by the empirical formula [21]:

$$L[\text{\AA}] = 250 \left(\frac{A}{\rho} \right) \left(\frac{E}{Z^{1/2}} \right)^n \quad (2)$$

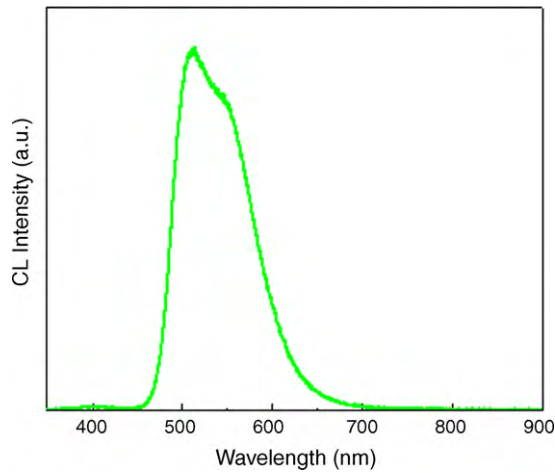


Fig. 5. CL spectra of $\text{Ca}_3\text{Sc}_2\text{Si}_3\text{O}_{12}:\text{Ce}^{3+}$ phosphor.

$$n = \frac{1.2}{1 - 0.29 \log_{10}^2} \quad (3)$$

where A is the atomic weight, ρ is the density, Z is the atomic number, and E is the accelerating voltage. For $\text{Ca}_3\text{Sc}_2\text{Si}_3\text{O}_{12}:\text{Ce}^{3+}$, the electron penetration depth at 2.5 kV is estimated to be 29 Å.

The dominant wavelength and color purity compared to the 1931 CIE Standard Source C illuminant [$C=(0.3101, 0.3162)$] for the phosphor were determined from the spectrum in Fig. 5. The dominant wavelength of a color is the single monochromatic wavelength of the spectrum whose chromaticity is on the same straight line as the sample point (x_s, y_s) and the illuminant point (x_i, y_i) as shown in Table 1. The color purity is the weighted average of the (x, y) coordinate relative to the coordinate of the illuminant and the coordinate of the dominant wavelength

$$\text{color purity} = \frac{\sqrt{(x_s - x_i)^2 - (y_s - y_i)^2}}{\sqrt{(x_d - x_i)^2 - (y_d - y_i)^2}} \times 100\% \quad (4)$$

where (x_d, y_d) is the color coordinate of the dominant wavelength. From the measured spectra, dominant wavelength and color purity are found to be about 552 nm and 67%, respectively.

Fig. 6 shows the PL decay curves of the phosphor fired at different temperatures. As shown in Fig. 6, the decay time of the phosphor, which attributes to the 5d–4f transitions of Ce^{3+} , depends on the firing temperature. The lifetime of the phosphor becomes longer with the increasing of the firing temperature. The plotting of decay curve can be well fitted by a double-exponential decay curve using an equation [22,23]:

$$I = A_1 e^{-t/\tau_1} + A_2 e^{-t/\tau_2} \quad (5)$$

where τ_1 and τ_2 are fast and slow components of the luminescent lifetime, respectively. A_1 and A_2 are corresponding fitting parameters. The fit curve and measured values of the phosphor fired at 1100 °C are shown in Fig. 7(a). The curve shows a fair consistency with the double-exponential decay, with $\tau_1 = 5.28$ ns and $\tau_2 = 50.89$ ns. The residuals of the decay curve and fit curve are evenly distributed about zero as shown in Fig. 7(b), which indicate the fit result is well.

Table 1

The color coordinates of the sample point, the dominant wavelength and the illuminant point.

x_s	y_s	x_d	y_d	x_i	y_i
0.3143	0.6705	0.3159	0.6791	0.3101	0.3162

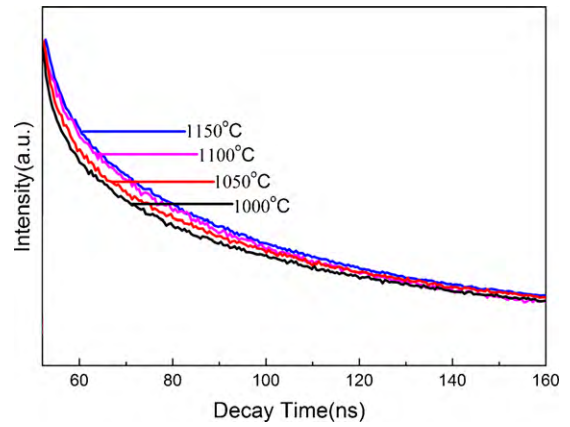


Fig. 6. PL decay curves of phosphors fired at different temperatures ($\lambda_{\text{ex}} = 460$ nm, $\lambda_{\text{em}} = 505$ nm).

The other decay times of phosphors fired at different temperature are shown in Table 2. The fit results also show that the lifetime of the phosphor increases with the increase of the firing temperature. The life time τ is described by the equation [24]

$$\tau = (\gamma_r + \gamma_{nr})^{-1} \quad (6)$$

where γ_r and γ_{nr} are the radiative rate and nonradiative rate, respectively. Since the grain of the sample grows up with the

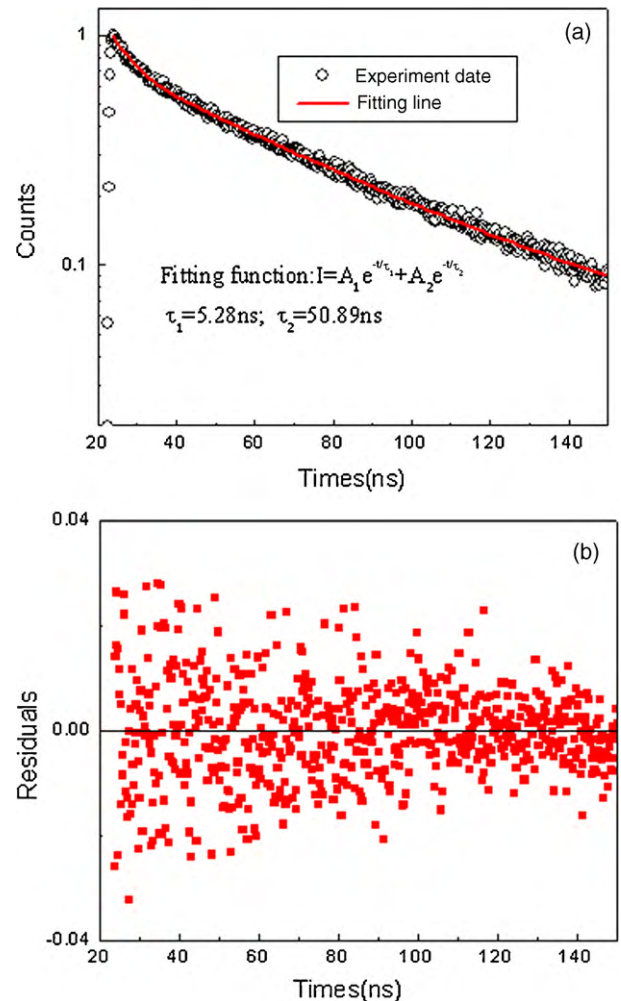


Fig. 7. The fit curve and measured values of the phosphor fired at 1100 °C.

Table 2
Decay times of phosphors fired at different temperatures.

Temperature (°C)	τ_1 (ns)	τ_2 (ns)
900	4.58	45.69
1000	4.85	47.34
1050	5.12	49.57
1100	5.28	50.89

increasing of firing temperature, the defects and nonradiative rate in the phosphor decrease. Therefore, the life time (τ) of the phosphor increases with the increasing of firing temperature as shown in Table 2.

4. Conclusions

$\text{Ca}_3\text{Sc}_2\text{Si}_3\text{O}_{12}:\text{Ce}^{3+}$ phosphors with single phase were successfully synthesized by a gel-combustion method. The samples with a sub-micron size and spherical grain fired at 1100 °C were obtained. The particle size of the phosphor increases with the increase of the firing temperature. The excitation spectra show a broad and strong absorption at about 460 nm. Bright green-emission located at 505 nm is observed, which is attributed to the characteristic emissions from 5d–4f transition of Ce^{3+} . The sample excited at low-voltage (2.5 kV) electron beam shows bright green CL, in which the dominant wavelength and color purity are found to be about 552 nm and 67%, respectively. The lifetime of the phosphor increases with the increasing of the firing temperature, results from the decrease in nonradiative rate under higher firing temperature.

Acknowledgments

The work described in this paper was supported by grants from the Ministry of Science and Technology of China Grant

(2006CB601104, 2006AA03A133), and the Research Grants Council of Hong Kong (Project No. PolyU 5004/07P), Hong Kong Polytechnic University Internal Grant (J-BB9R).

References

- [1] S. Nakamura, T. Mukai, M. Senoh, *Appl. Phys. Lett.* 64 (13) (1994) 1687–1689.
- [2] L.Y. Zhou, J.S. Wei, J.R. Wu, F.Z. Gong, L.H. Yi, J.L. Huang, *J. Alloys Compd.* 476 (2009) 390–392.
- [3] W.H. Hsu, M.H. Sheng, M.S. Tsai, *J. Alloys Compd.* 467 (2009) 491–495.
- [4] S.H. Lee, D.S. Jung, J.M. Han, H.Y. Koo, Y.C. Kang, *J. Alloys Compd.* 477 (2009) 776–779.
- [5] Q.Y. Shao, H.J. Li, Y. Dong, J.Q. Jiang, C. Liang, J.H. He, *J. Alloys Compd.* 498 (2010) 199–202.
- [6] Y. Shimomura, N. Kijima, US007189340 B2, 2007.
- [7] Y. Shimomura, T. Honma, M. Shigeiwa, T. Akai, *J. Electrochem. Soc.* 154 (2007) 35–38.
- [8] Y. Shimomura, T. Kurushima, M. Shigeiwa, N. Kijima, *J. Electrochem. Soc.* 155 (2008) 45–49.
- [9] Y.H. Liu, J.H. Hao, W.D. Zhuang, Y.S. Hu, *J. Phys. D: Appl. Phys.* 42 (2009) 245102.
- [10] Z.L. Wang, H.L.W. Chan, H.L. Li, J.H. Hao, *Appl. Phys. Lett.* 93 (2008) 141106.
- [11] J.H. Hao, J. Gao, *Appl. Phys. Lett.* 85 (2004) 3720–3722.
- [12] J.H. Hao, Z. Lou, I. Renaud, M. Cocivera, *Thin Solid Films* 467 (2004) 182–185.
- [13] B.L. Abrams, P.H. Holloway, *Chem. Rev.* (Washington, DC) 104 (2004) 5783–5801.
- [14] B.V. Mill, E.L. Belokoneva, M.A. Simonov, N.V. Belov, *J. Struct. Chem.* 18 (1977) 321–323.
- [15] K.Y. Jung, H.W. Lee, Y.C. Kang, S.B. Park, Y.S. Yang, *Chem. Mater.* 17 (2005) 2729–2734.
- [16] Y.C. Kang, S.B. Park, *J. Mater. Res.* 14 (1999) 2611–2615.
- [17] S. Shionoga, W.M. Yen, *Phosphor Handbook*, CRC Press, Boston, MA, 1999, p. 186.
- [18] Z.L. Wang, Z.W. Quan, P.Y. Jia, C.K. Lin, Y. Luo, Y. Chen, J. Fang, W. Zhou, C.J. O'Connor, J. Lin, *Chem. Mater.* 18 (2006) 2030–2037.
- [19] Y.H. Zhou, J. Lin, M. Yu, S.B. Wang, H.J. Zhang, *Mater. Lett.* 56 (2002) 628–636.
- [20] J.S. Wu, C.L. Jia, K. Urban, J.H. Hao, X.X. Xi, *J. Mater. Res.* 16 (2001) 3443–3450.
- [21] H. Wang, C.K. Lin, X.M. Liu, J. Lin, *Appl. Phys. Lett.* 87 (2005) 1–3, 181907.
- [22] S. Mukarami, H. Markus, R. Doris, M. Makato, *Inorg. Chim. Acta* 300–302 (2000) 1014–1021.
- [23] J. Hao, S.A. Studenikin, M. Cocivera, *J. Appl. Phys.* 90 (2001) 5064–5069.
- [24] W.W. Zhang, W.P. Zhang, P.B. Xie, M. Yin, H.T. Chen, *J. Colloid Interface Sci.* 262 (2003) 588–593.